

¹ Hardik B. Tank
² Dharmesh J. Shah

Low PAPR Filtered OFDM using Modified Selective Mapping



Abstract: - Wireless Communication has been witnessing generational change in the span of eight to ten years since it came in existence. From generation 1G to 3G and from 4G to 5G the telecommunication world has seen significant improvements along with enhanced performance with every passing year. The objective of research is to comprehensive study of Filtered Orthogonal Frequency Division Multiplexing (F-OFDM) as a promising waveform option for fifth-generation (5G) communications, distinguished by its capacity to suppress out-of-band emission (OOBE) and accommodate asynchronous transmission. Though there are many advantages but the challenge of a high peak-to-average power ratio (PAPR) among new waveform candidates can't be ignored. To address this problem, the selective mapping technique is used as a key method to alleviate the elevated PAPR trend within multicarrier systems. This research put emphasis on applying selective mapping technique to overcome the high PAPR values in an F-OFDM system with different windowed filters such as kaiser, Nuttles blackman harris and Root raised cosine followed by a proposed Modified Selective mapping technique for further improved performance in terms of PAPR for the Filtered OFDM for different window functions in comparison with the conventional OFDM system, SLM F-OFDM system. Furthermore, PAPR performance is evaluated for all the three-system using the different window techniques analyzed for both systems, both with and without the SLM technique and Modified SLM technique to mitigate the PAPR disadvantage of the Filtered OFDM system. Simulation results underscore that F-OFDM enhanced by SLM and MSLM outperforms OFDM across PAPR.

Keywords: Windowed methods, Fifth generation, Filtered OFDM, RRC window, Kaiser window, Nuttall's blackman-harris window, Peak-to-Average Power Ratio, Selective Mapping.

I. INTRODUCTION

The new age wireless communication systems represent a remarkable advancement beyond the present 4G LTE standards. These advancements in the wireless communication not only revolutionized mobile communication but also the transportation, medical, defence and security, pharmaceutical, high-speed vehicles, and diverse manufacturing industries. This surging demand for wireless services includes many aspects such as Massive Machine Communication (mMTC), Ultra Reliability and Low Latency (URLLC), and Enhanced Mobile Broadband (eMBB), as well as the seamless transmission of videos and real-time content delivery. One of the key drivers for the competition in fifth-generation technologies is IoT-based services. To achieve these ambitious targets, the next-generation technologies need to deliver high-speed broadband, exceptionally reliable connectivity, and ultra-low latency. Achieving lower communication latency is pushing us to upgrade the existing communication system to enhance data rates and spectral efficiency. The evolution to 5G standards includes the design and development of improved mobile communication channel models, amplification devices, modulation schemes, and encoding and decoding algorithms. These technological evaluations align with the goal to deliver the high standards set by 5G. In addition, addressing spectral efficiency concerns, the industry has proposed a novel radio waveform known as Filtered OFDM (F-OFDM), introduced by 3GPP. This proposed Filtered OFDM waveform influences the capacity to improve spectral efficiency by reducing out-of-band radiation, contributing to the overall improvement of communication systems.

Orthogonal Frequency Division Multiplexing is the widely accepted modulation technique in a wireless communications system because it lets control the inter-symbol interference and offers flexibility against frequency selective fading. As filtering increases the spectral efficiency and limits the out-of-band emissions, Filtered OFDM is the attempt to enhancing OFDM seeking to overcome its limitations via the filtering means [1]. F-OFDM radio waveform also has a potential to become a waveform contender for 5G systems. In particular, F-OFDM has a generally easier design, it also supports orthogonal transmission, and reduced PAPR complexity due to approaches

¹ * Department of Electronics and Communication, L.D. College of Engineering, Ahmedabad, Gujarat, India. Email: hbtank@ldce.ac.in

² Provost, Indrashil University, Mehsana, Gujarat, India.

Copyright © JES 2024 on-line : journal.esrgroups.org

described in the paper. Furthermore, the increased spectral efficiency, reduced computational complexity, and lower latency [2]. One novel method for waveforms modulation in wireless networks based on Universal Filtered Multicarrier, depending on the sub-band size, the sub-band filter configuration is modified to reduce interference and ICI or frequency selectivity. Filter length causes increased ICI and decreased ISCI, according to the investigations. In this method, the filter length is optimized and the symbol utilization and SINR are increased 1 to 3 dB [3]. Two aspects of research are presenting a simplified UFMC receiver structure. After receiving the UFMC symbol through 2N-point FFT and decimation, a simplified equivalent of the received symbol lies. Instead of the 2N-point FFT processor and decimator, the computational complexity is halved by using a single N-point FFT processor. Thus, the simplified UFMC receiver model appears to be almost an OFDM receiver [4].

Another challenging issue in OFDM systems is the Peak-to-Average Power Ratio limitation, as a result of high PAPR, signals can be prone to distortion and increases the system's power-efficiency consumption. Multiple methods have been proposed to resolve the PAPR problem with OFDM. As shown in, the Two-piecewise linear companding technique accurately reduces PAPR with a low computational effort compared to traditional companding methods [5]. The proposed PAPR reduction model in can be utilized for OFDM-Index Modulation systems as it reduces PAPR using phase rotation factors and variously rotates signals on selected partial sub-carriers [6]. Apparently, Selective mapping is a well-accepted method to reduce the PAPR in OFDM systems particularly in 5G systems. With nearly two decades, SLM has been studied and noticed and applied for various OFDM systems to combat the PAPR problems and developed a special SLM methods for the variants of them; Alamouti coded MIMO-OFDM system, downlink power domain OFDM-NOMA systems [7], UW-OFDM systems [8], wavelet-based cognitive radio for OFDM system [9], and non-coherent OFDM-IM system [10].

Selective mapping has been proven to be an efficient tool in combating PAPR problems in OFDM signals since it is fairly distortion less, has high PAPR reduction performance, and can be readily tailored to a diverse array of OFDM systems [11]. As a result, SLM has been suggested as a viable option for PAPR reduction, and a variety of investigations have demonstrated that SLM could be critical to enhancing the performance of forthcoming MIMO-OFDM systems and the functionality and system of Massive MIMO systems for the future generation wireless communication [12]. In addition, some different versions of SLM with different matrices such as the Walsh Hadamard and Riemann matrices have been recommended, and the most used one is as follows [13].

SLM is a notable and recognized PAPR reduction technique in OFDM, used to achieve both spectral and power efficiency, comparably to Partial Transmit Sequence (PTS) [14],[15]. For instance, SLM proved to be multi-dimensional as it adapted to different communication technologies that included visible light communication systems [16]. Overall, the research scenario highlights the importance of SLM in solving PAPR challenges in OFDM systems, and demonstrates its flexibility, efficiency and effectiveness to reduce PAPR and provide communication systems the performance improves, especially in the case of emerging technologies such as 5G networks.

II. FILTERED OFDM SYSTEM MODEL

Filtered Orthogonal Frequency Division Multiplexing (OFDM) is a key method for improving how efficiently we use spectrum and energy in upcoming wireless communication systems, particularly in networks beyond 5G. Moreover, the filtered OFDM can be represented as a variant of the family of evolved OFDM protocols such as the GFDM (Generalized Frequency Division Multiplexing) and the UF-OFDM (Universal Filtered OFDM) which anticipated a fundamental role on the evolution of mobile communications beyond fifth generation networks (5G) [17]. Additionally, there's ongoing research into new waveforms for 5G, considering the strengths and weaknesses of different options like OFDM and filter-bank multi-carrier (FBMC) [18]. Although OFDM has been widely used in previous communication systems, it might not meet the ambitious target set for 5G networks [19]. So, the new waves like Filter Bank Multi-Carrier (FBMC), Universal Filtered Multi-Carrier (UFMC), Generalized Frequency Division Multiplexing (GFDM) etc. are emerging. These alternatives are meant to be OFDM expansion and offers solutions to existing demand problems by 5G also Future networks [20].

Filtered Orthogonal Frequency Division Multiplexing (F-OFDM) is the possible waveform in which two filters are applied across the frequency spectrum, one for the transmitter and one for the receiver. Block diagram represents the F-OFDM concept as shown in figure 1. The F-OFDM signal in the transmitter is processed using OFDM before it reaches the transmitter filter in this system. At the receiver, the Filtered OFDM signal goes through a filter that matches the transmitter's filter, shaping the spectrum. This receiver filter helps block out unwanted signals from nearby sources, ensuring that the OFDM signal is protected from interference. Reducing the- high

out-of-band emission (OOBE) levels that are inherent to the OFDM system is the main goal of the transmitter's filter. This modification concurrently reduces latency and allows for asynchronous transmission. Consequently,

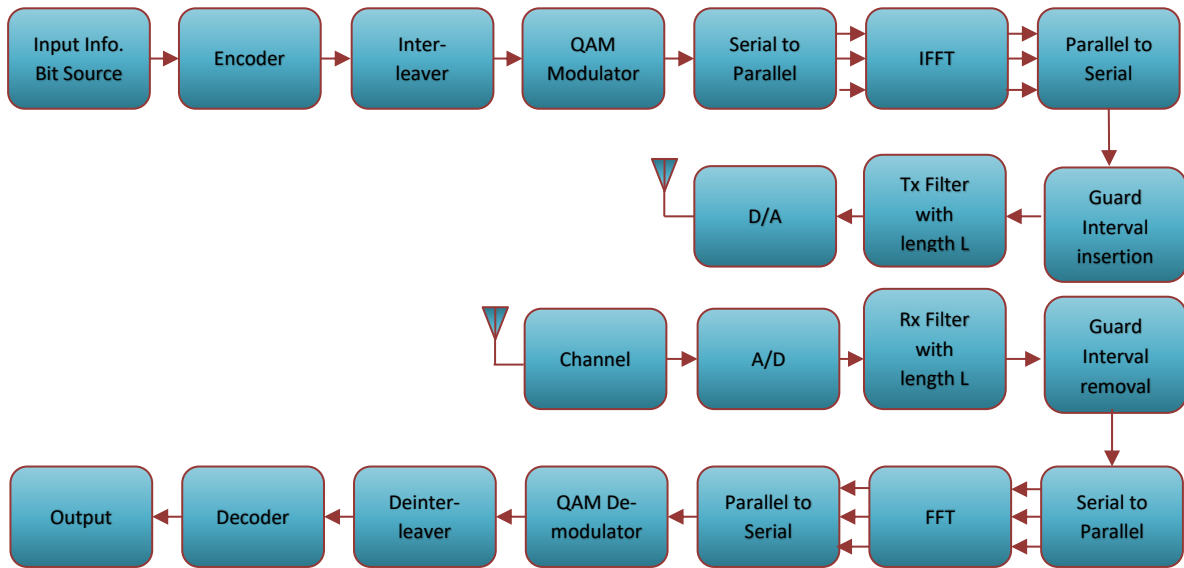


Figure 1: Filtered OFDM system model

this supports spectral efficiency, which is essential for fulfilling the requirements of 5G technology. Conversely, the architecture of the system becomes more complex as a result of the filter's integration.

Furthermore, the inclusion widens the power distribution among samples, which increases the Peak-to-Average Power Ratio (PAPR) as a result of the filter's effect. This ultimately causes the mean signal power to decrease, which worsens PAPR performance. Consequently, higher PAPR and a higher computational load on the system accompany the enhanced spectral efficiency of F-OFDM.

III. FILTER DESIGN

In the Filter OFDM section, designing of filter plays vital role in achieving dual goal of frequency localization of signal and increasing the flexibility between time and frequency localization. This focus on frequency-domain localization can lead to extensions in the time domain. In the next section, we present an example of a filter scheme that balances time and frequency localization to illustrate. This method uses a soft cut of the prototype filter, using a time-domain window with seamless transitions. In the OFDM system, the signal has a rectangular pulse pattern that is reminiscent of a windowed sinc function. This reasons significant aspect lobes on each end of the signal's frequency area, which lead to suboptimal frequency spectrum localization. A foremost desire on this research is a sinc impulse reaction clear out, essentially a low-pass filter (LPF), due to its potential in suppressing Out-of-Band Emission (OOBE).

The Filter preserves the pass band integrity of the signal. Additionally, the application of a time windowing mask is implemented to improve time localization and ensure smooth transitions at both ends of the filter's impulse response in time domain. The final finite impulse response (FIR) filter named windowing sync filter is obtained by multiplying the sync function by three different window functions: Kaiser, Nuttall's Blackman Harris and Routed Raised Cosine (RRC), finite one -Time-zone window it further enhances performance. A windowing-sync filter, also known as a final finite impulse response (FIR) filter, is constructed by multiplying the sync functions by window functions: Kaiser, Nuttall's Blackman Harris, and rooted raised cosine (RRC), finite-time -1. Region windows for greater efficiency.

As a result, the filter's bandwidth can be defined as the collective frequency span that includes the allocated subcarriers. Furthermore, the use of windowing in the truncated filter response ensures a reasonable level of time localization. Due to increased bandwidth of both transmission (Tx) and reception (Rx) filters in comparison to subcarrier spacing, the primary temporal extent of the end-to-end time domain filter is significantly shorter than the OFDM symbol length. Furthermore, this extent is quite smaller than the Cyclic Prefix (CP) length when the filter's tail forms the side lobe and the filter's head does not result in an overhead.

As a consequence, the time-domain sinc impulse response filter can be mathematically expressed as:

$$F(n) = w(n) * LPF(n) \tag{1}$$

where LPF(n) represents the sinc impulse response filter.

In the given context,

(1) Kaiser window function is represented as:

$$ksr(n) = \frac{I\left(\beta \sqrt{1 - \left(\frac{n - \frac{M}{2}}{\frac{M}{2}}\right)^2}\right)}{I(\beta)}. \quad 0 \leq n \leq M \tag{2}$$

beta= 0.5. The length of the window is N = M + 1. For the designing of an FIR filter with side lobe attenuation of α dB, the Kaiser window function should be implemented by using the following β.

$$\beta = \begin{cases} 0.1102(\alpha - 8.7), & \alpha > 50 \\ 0.58(\alpha - 21)^{0.4} + 0.078(\alpha - 21), & 50 \geq \alpha \geq 21 \\ 0, & \alpha < 21 \end{cases}$$

The increment in value of β will increase the width of the main lobe and reduces the amplitude of the side lobes as well thereby increases the attenuation.

(2) Nuttall's Blackman-Harris window function is represented as:

$$nutl(n) = a - b \cdot \cos\left(\frac{2\pi n}{M-1}\right) + c \cdot \cos\left(\frac{4\pi n}{M-1}\right) - d \cdot \cos\left(\frac{6\pi n}{M-1}\right), n = 0, 1, 2, \dots, M - 1 \tag{3}$$

The following equation defines the periodic Nuttall four-term Blackman-Harris window.

$$nutl(n) = a - b \cdot \cos\left(\frac{2\pi n}{M}\right) + c \cdot \cos\left(\frac{4\pi n}{M}\right) - d \cdot \cos\left(\frac{6\pi n}{M}\right), n = 0, 1, 2, \dots, M - 1 \tag{4}$$

The periodic window is N-periodic.

The window coefficients are, a = 0.363, b = 0.48, c = 0.136, d = .0106.

(3) RRC window function is represented as:

$$rrc(n) = \left[0.5 \left\{1 - \cos\left(\frac{2\pi n}{M-1}\right)\right\}\right]^\alpha \tag{5}$$

where "α" serves as the roll-off factor. This parameter determines the shape of the window, with the constraint 0 < α < 1. To achieve greater flexibility in filter design and a harmonious balance of time and frequency localization, the length of the F-OFDM filter is allowed to surpass the length of the Cyclic Prefix (CP). This augmented filter length improves the design's flexibility. In this context, the F-OFDM filter must meet key criteria such as transition sharpness, passband flatness, and stopband attenuation. On the other hand, increasing the filter setting results in complexity. Consequently, it is prudent to increase the length of the filter above a certain threshold to reduce complexity.

The RRC window's roll-off factor adds an additional layer of control to create a solid balance of time and frequency localization. However, this window must have smooth transitions at both ends to avoid sudden spikes at the start and end of the truncated filter. This technique blocks unintended frequency spillover in the truncated filter. thus, the roll-off factor emerges as an important parameter for shaping the window, providing additional flexibility for coordinating time and frequency localization, as a result of its advantageous characteristics, the RRC window is better suited for OFDM system filtering than other windows.

IV. PAPR PROBLEM

Usually, multicarrier systems such as Orthogonal frequency division multiplexing, the baseband signal is directed to the Inverse Fast Fourier Transform (IFFT) unit, which modulates the subcarriers with data symbols. Consequently, the OFDM signal is represented by:

$$O_{fdm}(n) = \frac{1}{\sqrt{NP}} \sum_{k=0}^{NP-1} O_{kfdm} e^{-\frac{j2\pi kn}{NP}} \quad \text{for } 0 \leq n \leq NP - 1 \tag{6}$$

In the given equation, $O_{fdm}(n)$ refers to the complex block data of the M subcarriers after constellation mapping. This factor is chosen as a multiple of the Nyquist rate to ensure precise computation of Peak-to-Average Power Ratio (PAPR) values. Time domine OFDM signal is generated by simultaneously applying the IFFT operation to the subcarriers. These subcarriers are differentiated by their independence and different phases.

Occasionally, the subcarriers' phases coincide in the same direction, resulting in a higher peak power than the signal's average. Consequently, The PAPR of an OFDM signal is the ratio of the maximum peak power, $|O_{fdm}(n)|^2$, to the average power of the signal, $E\{|O_{fdm}(n)|^2\}$

$$PAPR = \frac{Max |O_{fdm}(n)|^2}{E\{|O_{fdm}(n)|^2\}} \tag{7}$$

In the equation, the complementary cumulative distribution function (CCDF) is commonly used to assess the likelihood of the signal's Peak-to-Average Power Ratio (PAPR) surpassing a particular threshold value ($PAPR_0$).

$$\begin{aligned} CCDF &= Pr(PAPR \geq PAPR_0) \\ &= 1 - (1 - e^{-PAPR_0})^{NP} \end{aligned} \tag{8}$$

V. SELECTIVE MAPPING TECHNIQUE FOR FILTERED OFDM

The higher Peak-to-Average Power Ratio (PAPR) is a possible difficulty for the F-OFDM system. The presence of a transmitter filter causes a broader distribution of power across samples because the filter length exceeds the cyclic prefix (CP) period; as a result, the mean power of the signal decreases, causing a significant expansion in the gap between the maximum peak power and the mean power of the F-OFDM signal. Therefore, the F-OFDM system outperforms the standard OFDM system in terms of PAPR. In this study, three windowed filters are evaluated for the targeted parameter, PAPR, in terms of OFDM signal, so that the best filter can be selected based on simulation results in terms of PAPR, power spectral density, and system complexity.

The traditional Selective Mapping (SLM) technique involves creating multiple data blocks with the same information, which are then array-multiplied by different phase vectors, as depicted in figure 2. The sequence with the lowest Peak-to-Average Power Ratio (PAPR) is chosen for transmission. Each data block is multiplied by W different phase sequences, each of length N and designated as $W(u)$, yielding N new (modified) data blocks. The input data is available in each data block Y of length N . The data blocks are then multiplied factor by factor using a phase sequence.

$$W^{(u)} = [W_{u,0}, W_{u,1}, \dots, W_{u,N-1}]^N, u = 0, 1 \dots, U \tag{9}$$

Resulting in U transformed data blocks,

$$\begin{aligned} Y^{(u)} &= [Y_{u,0}, Y_{u,1}, \dots, Y_{u,N-1}]^N \\ \text{where, } Y_{u,k} &= Y_k W_{u,k}, \quad k = 0, 1 \dots, N - 1 \end{aligned} \tag{10}$$

After that, the N -point IFFT of each data block is performed; the resulting signal is provided as:

$$y^u(n) = \frac{1}{N} \sum_{k=0}^{N-1} Y_k W_{u,k} e^{(j2\pi kn/N)}, n = 0, 1 \dots, U - 1 \tag{11}$$

Pseudo random sequence is randomly generated exponential sequences, which is defined as:

$$W^u = e^{j\Phi u} \text{ where } \Phi u \in [0, 2\pi] \tag{12}$$

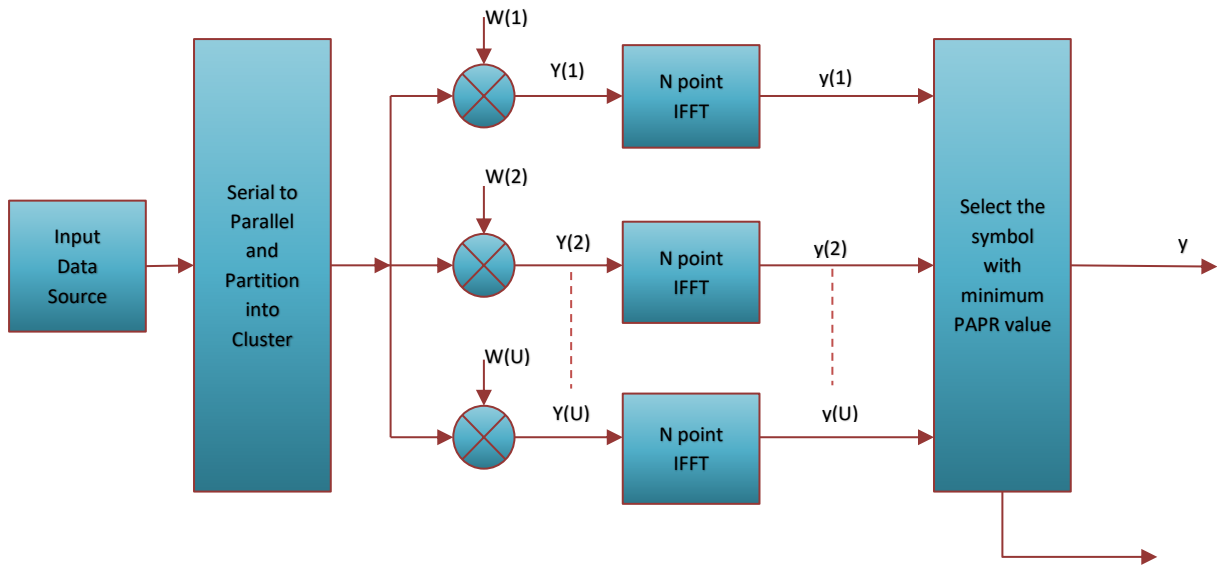


Figure 2: Selective Mapping Filtered OFDM system model

This section compares OFDM and F-OFDM waveforms using and without selective mapping techniques. The evaluation considers peak-to-average power ratio (PAPR) performance and frequency localization. The simulation frame parameters are defined as follows: N is set to 3000 in order to meet 5G requirements, and U is set to 2 to 32 to analyze the performance of the SLM technique with different phase sequences. For the F-OFDM case, a Low-Pass Filter (LPF) and three windowing masks are used to compare the results: Kaiser, Nuttall's Blackman Harris, and Rooted Raised Cosine (RRC) with a roll-off factor of value 0.6. To evaluate the PAPR, the Complementary Cumulative Distribution Function (CCDF) is considered across 3000 sub frames for both OFDM and F-OFDM; other simulation parameters are listed in the table below for the 5G scenario.

5.1. Simulation PAPR Performance

This subsection assesses the Peak-to-Average Power Ratio (PAPR) performance of OFDM and F-OFDM, with a focus on the Selective Mapping (SLM) method. To meet the 5G requirement of having a system bandwidth of 200 MHz and a subcarrier spacing of 60kHz, the system can handle a total of 3333 subcarriers; however, some of the subcarriers are used for guard intervals, so the effective number of carriers for the system on which the PAPR performance for SLM technique is carried out is 3000 sub carriers.

TABLE 1. F-OFDM Simulation specifications

Parameters	Values
Multi-carrier modulation schemes	OFDM, F-OFDM
F-OFDM IFFT/FFT length	2048
Modulation	256-QAM
Number of active subcarriers	3000
Order of the Filter	512, 1024
Subcarrier spacing	60 kHz
Channel	AWGN
F-OFDM symbol duration	16.67 μ s
CP duration	1.17 μ s
F-OFDM symbol duration with CP	17.84 μ s
Bandwidth	200 MHz

The simulation resolution in the figure 3 shows that the PAPR for the Kaiser window function at the clip rate 10^{-4} for the OFDM without filter is 12.81dB. For F-OFDM with the Kaiser window function, the PAPR increased up to 14.97dB with a 2.16dB increase. Similarly, for the Nuttall's Blackman Harris window function

shown in the figure 4, the PAPR is 14.92dB, which is increased by 2.11dB, and for the RRC window function PAPR for F-OFDM is 14.89dB shown in the figure 6, which is 2.08dB higher than that of OFDM. To overcome this increased PAPR for all the three-window functions, we implemented the conventional selective mapping technique, in which the number of phase sequence plays a vital role in the performance of PAPR. We can see from the simulation results from the figure for the all three windows that if we keep on increasing the U (number of phase sequences), we can observe the drastic decreased PAPR, but this improved performance comes at the cost of an increase in system complexity. We can also see from the results that after U=16, there is no search huge decrement in PAPR value. It has been observed from the simulation results that the PAPR values for SLM-OFDM and SLM-F-OFDM (for U=16) stand at 9.83dB and 11.59dB respectively for Kaiser window, 11.53dB for SLM-F-OFDM (for U=16) with Nuttall's Blackman Harris window and 11.23dB for the SLM-F-OFDM (for U=16) with RRC window.

The longer length of the filter in the F-OFDM waveform contributes to a lower mean power when compared to the OFDM standard. As a result, the difference between the peak amplitude and the signal's mean value widens, resulting in decline PAPR performance. The SLM approach minimizes correlation among samples within subblocks, which alters sample phases. This adjustment minimizes the signal's peak amplitude, hence improving PAPR performance. As a result, both analysis and simulation demonstrate that the F-OFDM waveform candidate has a high PAPR, affecting the efficiency of the transmitter's power amplifier. However, effective solutions such as SLM can be utilized to address this issue, potentially resulting in a PAPR decrease of more than 3 dB over the original system.

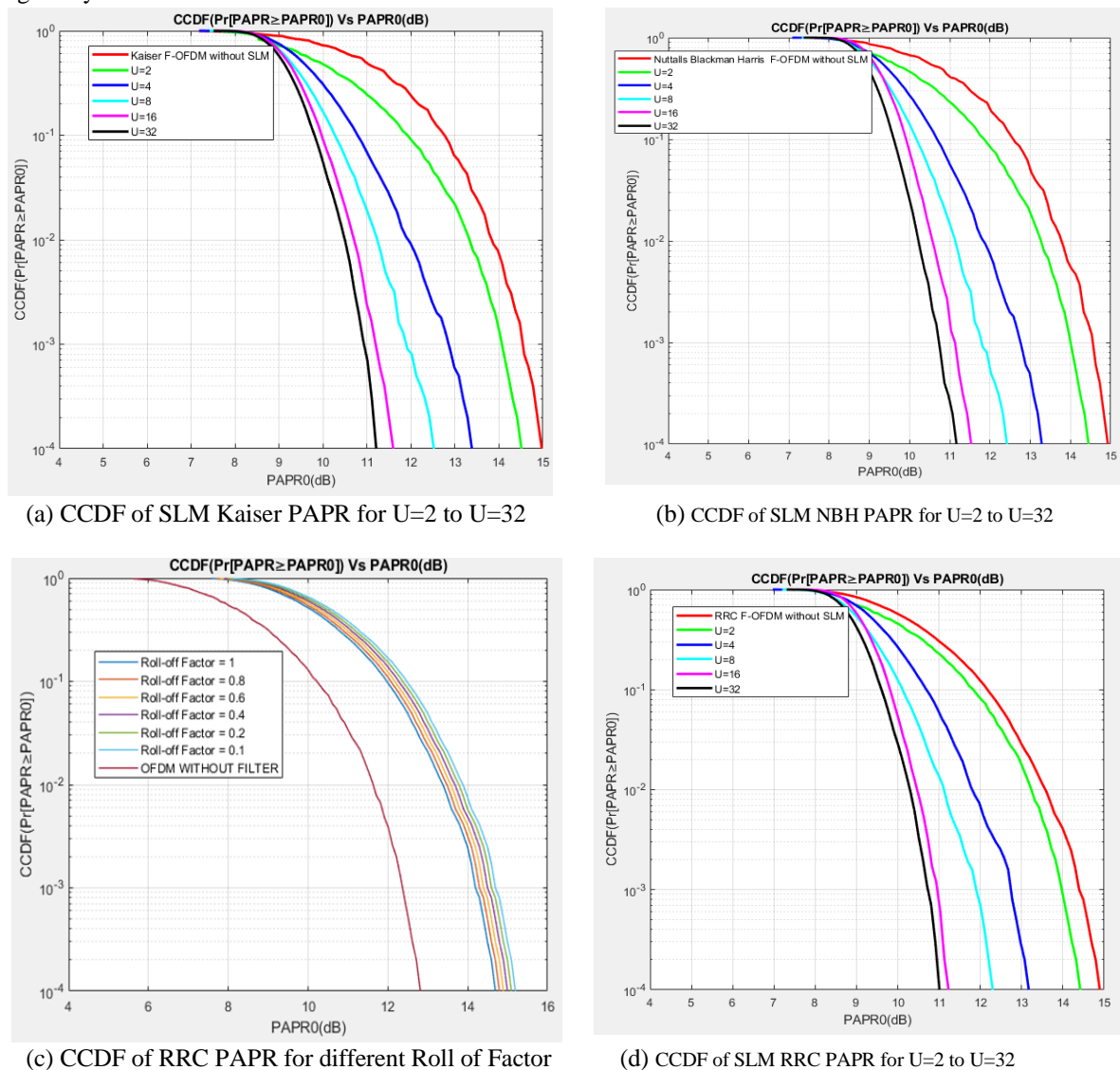


Figure 3: CCDF of SLM using different window function PAPR for U=2 to U=32

TABLE 2. SLM PAPR at Clip Rate 10^{-4}

	Kaiser FOFDM without SLM 14.97 dB	Nuttall's Blackman Harris FOFDM without SLM 14.92 dB	RRC FOFDM without SLM 14.89 dB
No. of Phase Sequences	Kaiser FOFDM with SLM	Nuttall's Blackman Harris FOFDM with SLM	RRC FOFDM with SLM
U=2	14.51 dB	14.44 dB	14.41 dB
U=4	13.38 dB	13.28 dB	13.17 dB
U=8	12.52 dB	12.41 dB	12.29 dB
U=16	11.59 dB	11.53 dB	11.23 dB
U=32	11.20 dB	11.16 dB	11.00 dB

VI. MODIFIED SELECTIVE MAPPING TECHNIQUE FOR FILTERED OFDM

The Discrete Sine Transform (DST) is a mathematical transformation that is closely related to the Fourier transform, much like the Discrete Fourier Transform (DFT). However, the DST employs a matrix made up entirely of real values. It corresponds to the imaginary components of a DFT that are approximately twice the length. This operation is performed on real data with odd symmetry. DSTs are widely used to solve partial differential equations with spectral methods. The various DST implementations produce slightly different odd/even boundary conditions

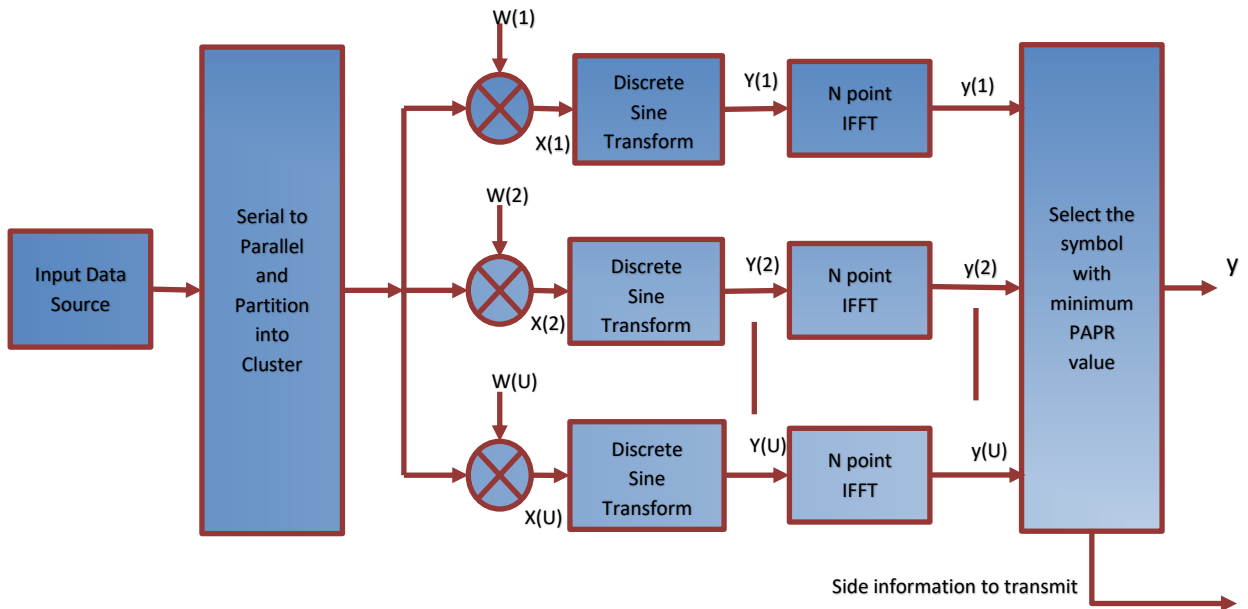


Figure 4: Modified Selective Mapping Filtered OFDM system model

at the array's two ends. There are several versions of the DST, each with slight adjustments in their definition. In this context, we consider DST-I, also known as DST.

The DST is given by:

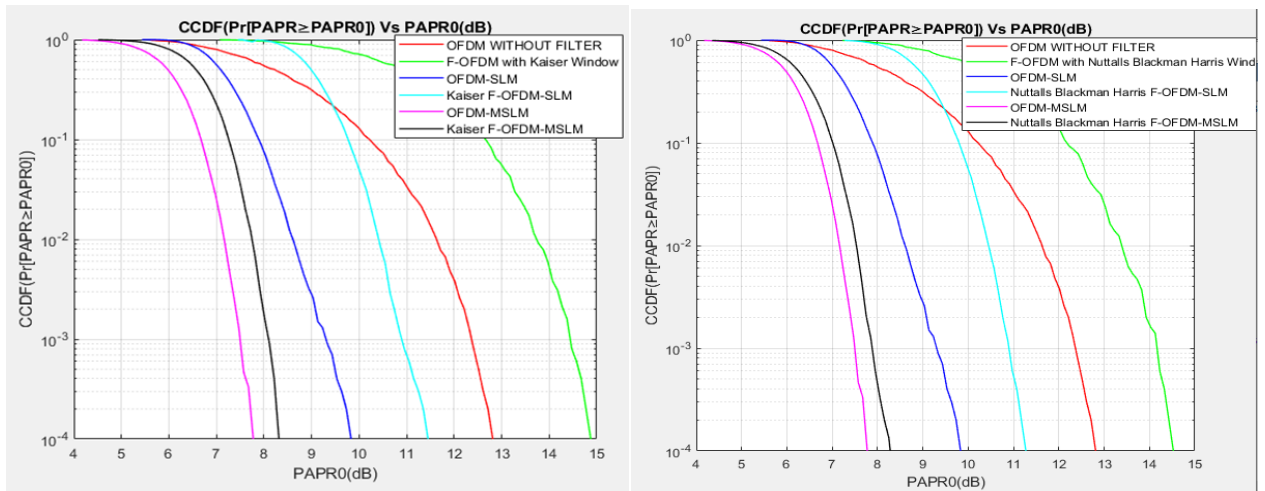
$$y(k) = \sum_{n=1}^N x(n) \sin\left(\frac{k\pi n}{N+1}\right), k = 1, 2, \dots, N \tag{13}$$

The inverse DST (IDST) is given by:

$$x(n) = \frac{2}{N+1} \sum_{k=1}^N y(k) \sin\left(\frac{k\pi n}{N+1}\right), n = 1, 2, \dots, N \tag{14}$$

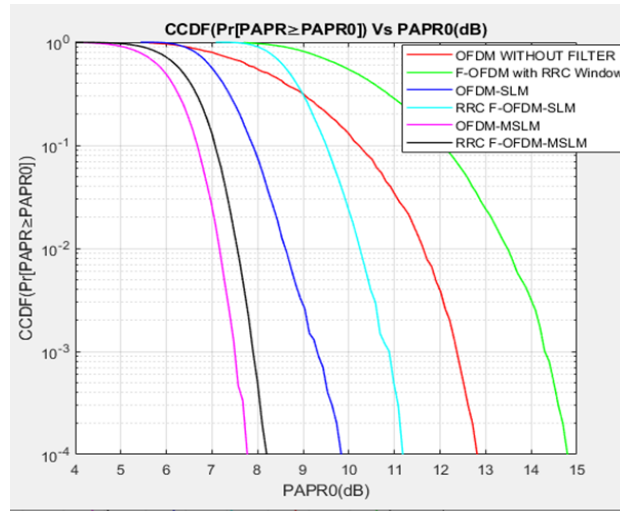
The collection of complex exponential functions is not the exclusive orthogonal foundation for generating baseband single-carrier signals. A single set of cosine and sine functions can also be utilized to provide an orthogonal basis, making the single-carrier system simpler to implement. As shown in Figure the transceiver block diagram of the MSLM system the transmitter starts by encoding the input data sequence for the "u-th" user. Following that, the coded bits are converted into multilevel symbols using modulation formats such as quadrature phase shift keying (QPSK) and 256-quadrature amplitude modulation (256QAM). These modulated symbols are then divided into blocks of N symbols and subjected to an N-point Discrete Sine Transform (DST). The subcarrier mapping step distributes DST outputs across $M (\geq N)$ designated subcarriers for transmission, leaving any unused

subcarriers with zeros. Following an M-point Inverse Discrete Sine Transform (IDST) operation, a cyclic prefix (CP) is added to the beginning of the IDST outputs.



(a) CCDF plot for Kaiser Window

(b) CCDF plot for NBH Window



(c) CCDF plot for RRC Window

Figure 5: CCDF of SLM-MSLM using different window function with comparison

TABLE 3. Simulation Summary of PAPR at Clip Rate 10^{-4}

	Kaiser Filter	NBH Filter	RRC Filter
OFDM without Filter	12.81 dB	12.81 dB	12.81 dB
F-OFDM with Filter	14.97 dB	14.92 dB	14.89 dB
OFDM - SLM	9.83 dB	9.83 dB	9.83 dB
FOFDM with SLM (U=16)	11.59 dB	11.53 dB	11.23 dB
OFDM-MSLM	7.77 dB	7.77 dB	7.77 dB
FOFDM with MSLM (U=16)	8.35 dB	8.18 dB	7.82 dB

It has been observed from the simulation results that the PAPR values for SLM-OFDM and SLM-F-OFDM (for U=16) stand at 9.83dB and 11.59dB respectively for Kaiser window, 11.53dB for SLM-F-OFDM (for U=16) with Nuttall's Blackman Harris window and 11.23dB for the SLM-F-OFDM (for U=16) with RRC window. And further more using the proposed modified selective mapping the PAPR performance for the OFDM with MSLM is 7.77dB now with the filtering techniques using Kaiser window PAPR at clip rate 10^{-4} is 8.35 (For U=16, with Nuttall's Blackman Harris window MSLM-F-OFDM (for U=16) is 8.18dB and for RRC window (for U=16) is 7.82dB, which is almost nearer to the OFDM system PAPR performance to compensate the increased PAPR value.

VII. CONCLUSION AND FUTURE WORK

The primary goal of this research work is to emphasize the PAPR performance of the Filtered OFDM waveform framework, which is being explored as an option for 5G and beyond 5G. The PAPR performance of F-OFDM using the SLM approach is assessed and compared with SLM-OFDM. The simulation findings show that the SLM technique reduces Filtered OFDM's PAPR by nearer 3 dB, The fundamental disadvantage of using the SLM approach to F-OFDM is the increased computing complexity of the system caused by the extra filter Furthermore, in the SLM we proposed the modified SLM using DST to analysed the PAPR performance and simulation results shows that it reduces PAPR to almost OFDM level which will mitigate the disadvantage of filtering produced for the PAPR. therefore, the F-OFDM framework based on the DST-SLM technique is an appropriate waveform design for 5G in terms of PAPR reduction performance, considering the balance of computational complexity and performance. In our future study, we want to focus on reducing the computational complexity of DST-SLM-F-OFDM without compromising performance.

REFERENCES

- [1] X. Yang, S. Yan, X. Li, and F. Li, "A unified spectrum formulation for OFDM, FBMC, and F-OFDM," *Electron.*, vol. 9, no. 8, pp. 1–15, 2020, doi: 10.3390/electronics9081285.
- [2] Y. A. Al-Jawhar, K. N. Ramli, M. A. Taher, N. S. M. Shah, S. A. Mostafa, and B. A. Khalaf, "Improving PAPR performance of filtered OFDM for 5G communications using PTS," *ETRI J.*, vol. 43, no. 2, pp. 209–220, 2021, doi: 10.4218/etrij.2019-0358.
- [3] R. Manda, A. Kumar, and R. Gowri, "Optimal filter length selection for universal filtered multicarrier systems," *Int. J. Eng. Trans. B Appl.*, vol. 36, no. 7, pp. 1322–1330, 2023, doi: 10.5829/ije.2023.36.07a.13.
- [4] R. Manda and R. Gowri, "Universal Filtered Multicarrier Receiver Complexity Reduction to Orthogonal Frequency Division Multiplexing Receiver," *Int. J. Eng. Trans. A Basics*, vol. 35, no. 4, pp. 725–731, 2022, doi: 10.5829/ije.2022.35.04a.12.
- [5] M. Al-Gharabally, A. F. Almutairi, and A. Krishna, "Performance Analysis of the Two-Piecewise Linear Companding Technique on Filtered-OFDM Systems," *IEEE Access*, vol. 9, pp. 48793–48802, 2021, doi: 10.1109/ACCESS.2021.3068371.
- [6] S. Y. Zhang and H. Zheng, "A Hybrid PAPR Reduction Scheme in OFDM-IM Using Phase Rotation Factors and Dither Signals on Partial Sub-Carriers," *Entropy*, vol. 24, no. 10, pp. 1–17, 2022, doi: 10.3390/e24101335.
- [7] M. Mounir, M. I. Youssef, and A. M. Aboshosha, "Low-complexity selective mapping technique for PAPR reduction in downlink power domain OFDM-NOMA," *EURASIP J. Adv. Signal Process.*, vol. 2023, no. 1, 2023, doi: 10.1186/s13634-022-00968-y.
- [8] M. Rajabzadeh and H. Steendam, "Precoding for PAPR Reduction in UW-OFDM," *IEEE Commun. Lett.*, vol. 25, no. 7, pp. 2305–2308, 2021, doi: 10.1109/LCOMM.2021.3068853.
- [9] K. R. Arjun and T. P. Surekha, "Peak-to-average power ratio reduction in wavelet based OFDM using modified selective mapping for cognitive radio applications," *Walailak J. Sci. Technol.*, vol. 18, no. 12, 2021, doi: 10.48048/wjst.2021.19814.
- [10] S. Gopi and S. Kalyani, "An Optimized SLM for PAPR Reduction in Non-Coherent OFDM-IM," *IEEE Wirel. Commun. Lett.*, vol. 9, no. 7, pp. 967–971, 2020, doi: 10.1109/LWC.2020.2976935.
- [11] K. H. Kim, "On the Phase Sequences and Permutation Functions in the SLM Scheme for OFDM-IM Systems," *IEEE Access*, vol. 8, no. Im, pp. 121733–121743, 2020, doi: 10.1109/ACCESS.2020.3007377.
- [12] B. DamodharTimande and M. K. Nigam, "PAPR reduction an effective approach for next frontier MIMO-OFDM systems," *J. Eng. Res.*, vol. 11, no. 1, pp. 223–231, 2021, doi: 10.36909/JER.11379.
- [13] S. R. Abdulridha and F. S. Hasan, "Enhanced SLM based OFDM-DCSK communication system for PAPR reduction," *Bull. Electr. Eng. Informatics*, vol. 11, no. 1, pp. 567–574, 2022, doi: 10.11591/eei.v11i1.3549.
- [14] A. J. Basha, M. R. Devi, S. Lokesh, P. Sivaranjani, D. M. Hussain, and V. Padhy, "PSO-DBNet for Peak-to-Average Power Ratio Reduction Using Deep Belief Network," *Comput. Syst. Sci. Eng.*, vol. 45, no. 2, pp. 1483–1493, 2023, doi: 10.32604/csse.2023.021540.
- [15] S. R. Abdulridha and F. S. Hasan, "Palm Clipping and Nonlinear Companding Techniques Based Papr Reduction in Odfm-Dcsk System," *J. Eng. Sustain. Dev.*, vol. 25, no. 4, pp. 84–94, 2021, doi: 10.31272/jeasd.25.4.8.
- [16] S. P. Valluri and S. Member, "for Visible Light Systems," 2020, [Online]. Available: <https://ieeexplore.ieee.org/iel7/6287639/8948470/08964378.pdf>
- [17] L. Deng, L. Deng, Y. M. Huang, Q. Chen, Y. He, and X. Sui, "Collaborative Blind Equalization for Time-Varying OFDM Applications Enabled by Normalized Least Mean and Recursive Square Methodologies," *IEEE Access*, vol. 8, pp. 103073–103087, 2020, doi: 10.1109/ACCESS.2020.2999387.
- [18] E. K. Hong *et al.*, "6G R&D Vision: Requirements and Candidate Technologies," *J. Commun. Networks*, vol. 24, no. 2, pp. 232–245, 2022, doi: 10.23919/JCN.2022.000015.
- [19] U. Farooq, P. Valsalan, N. Ul Hasan, and M. Zghaibeh, "a Noma-Ufmc Precoded System for 6G," *Azerbaijan J. High Perform. Comput.*, vol. 4, no. 2, pp. 188–197, 2021, doi: 10.32010/26166127.2021.4.2.188.197.

- [20] J. Kassam *et al.*, "Two-step multiuser equalization for hybrid mmwave massive MIMO GFDM systems," *Electron.*, vol. 9, no. 8, pp. 1–19, 2020, doi: 10.3390/electronics9081220.